

Electronic Supplementary Information

Soft Template-Mediated Coupling Construction of Sandwiched Mesoporous PPy/ Ag Nanoplates for Rapid and Selective NH₃ Sensing

Facai Wei^{†a}, Yonghui Zhong^{†a}, Hao Luo^{†a}, Yong Wu^a, Jianwei Fu^b, Qingguo He^c, Jiangong Cheng^c, Jongbeom Na^{*d}, Yusuke Yamauchi^{*[dedef](#)} and Shaohua Liu^{*ac}

^a State Key Laboratory of Precision Spectroscopy; Engineering Research Center of Nanophotonics & Advanced Instrument, Ministry of Education, School of Physics and Electronic Science, East China Normal University, Shanghai, 200241, P.R. China. E-mail: shliu@phy.ecnu.edu.cn

^b School of Materials Science and Engineering, Zhengzhou University, 75 Daxue Road, Zhengzhou, 450052, P. R. China

^c State Key Lab of Transducer Technology, Shanghai Institute of Microsystem and Information Technology, Chinese Academy of Science, Shanghai 200050, P. R. China

^d-[School of Chemical Engineering and](#) Australian Institute for Bioengineering and Nanotechnology (AIBN)[\)](#) and [School of Chemical Engineering](#), The University of Queensland, Brisbane, QLD 4072, Australia E-mail: j.na@uq.edu.au, y.yamauchi@uq.edu.au

^e JST-ERATO Yamauchi Materials Space-Tectonics Project, Kagami Memorial Research Institute for Materials Science and Technology, Waseda University, 2-8-26 Nishiwaseda, Shinjuku-ku, Tokyo 169-0051, Japan.-

^f [JST-ERATO Yamauchi Materials Space-Tectonics Project and International Center for Materials Nanoarchitectonics \(WPI-MANA\)](#), National Institute for Materials Science (NIMS), 1-1 Namiki, Ibaraki, Tsukuba 305-0044, Japan.

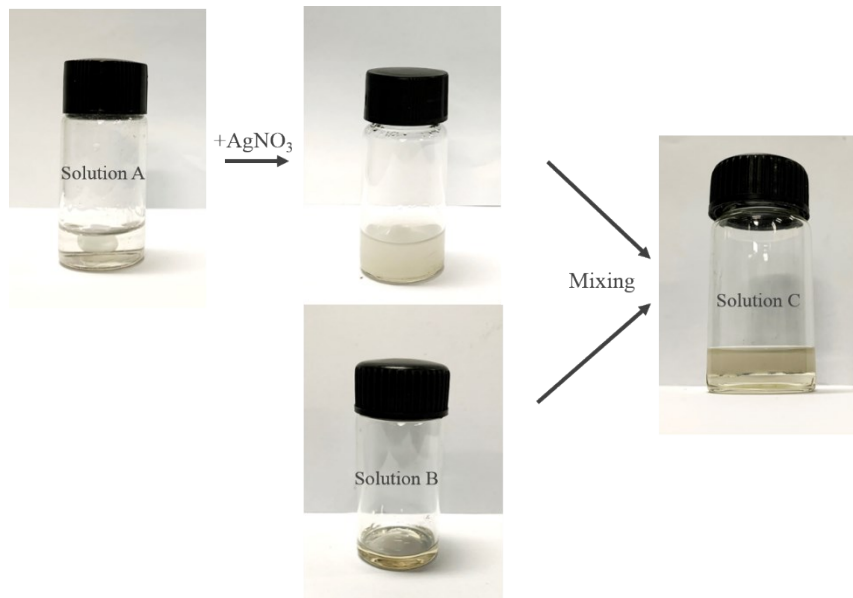


Fig. S1. Digital photos of the assembly process. Solution A is the aqueous phase, BCP is dissolved in THF/H₂O to form micelles and silver nitrate is then added to form turbidity phase. Solution B is the organic phase, a certain amount of pyrrole is dissolved in chloroform. Two solutions are mixed to spontaneously form the interface of solution C.

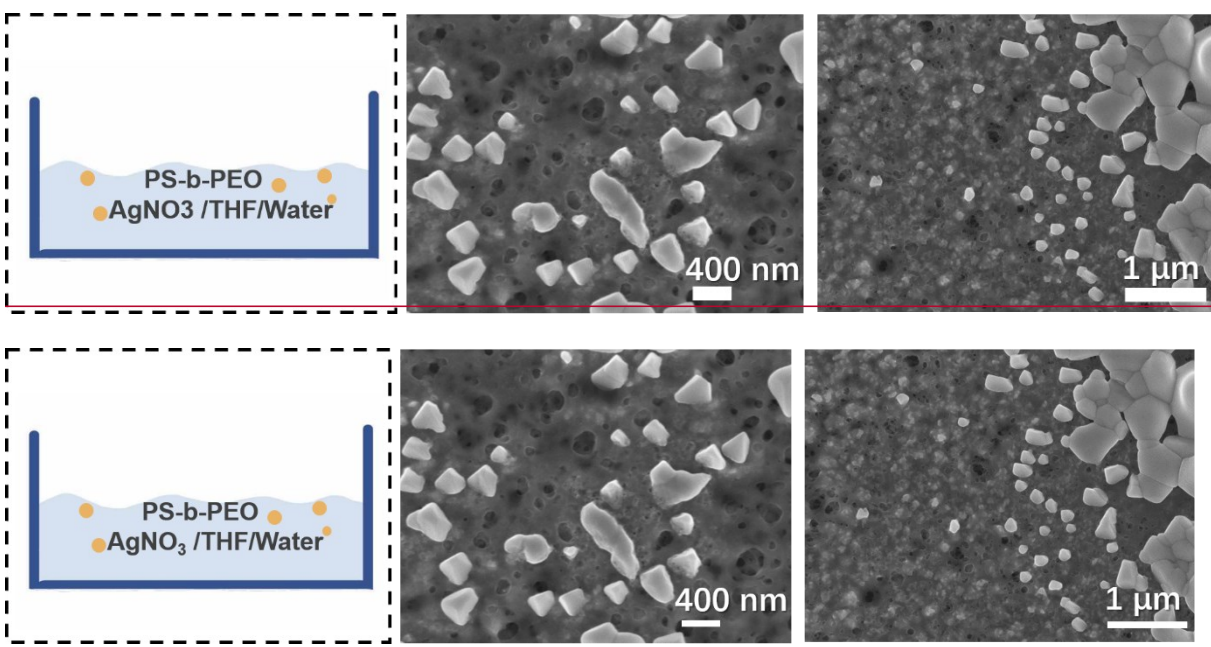


Fig. S2. Schematic diagram and SEM images of the BCP- Ag^+ chelate. The irregular morphology of the BCP- Ag^+ chelates indicated that the unique composite was formed by secondary growth upon the oxidation-reduction reaction, rather than direct growth based on the chelate particles.

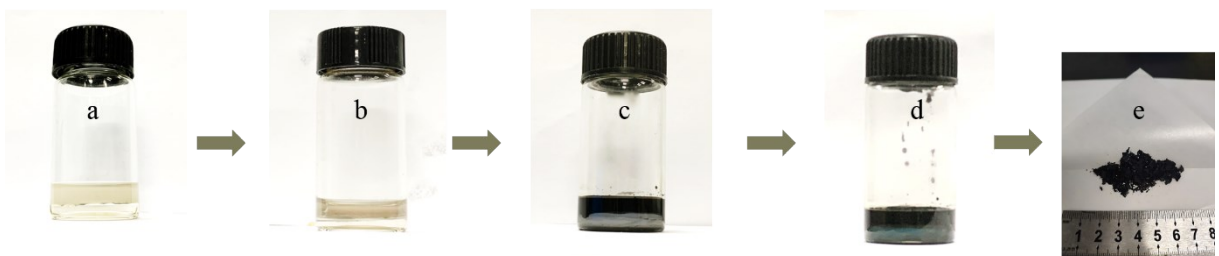


Fig. S3. Digital photos of the synthesis process after a) 0 h, b) 2 h, c) 12 h, d) 72 h and e) the resulting film products.

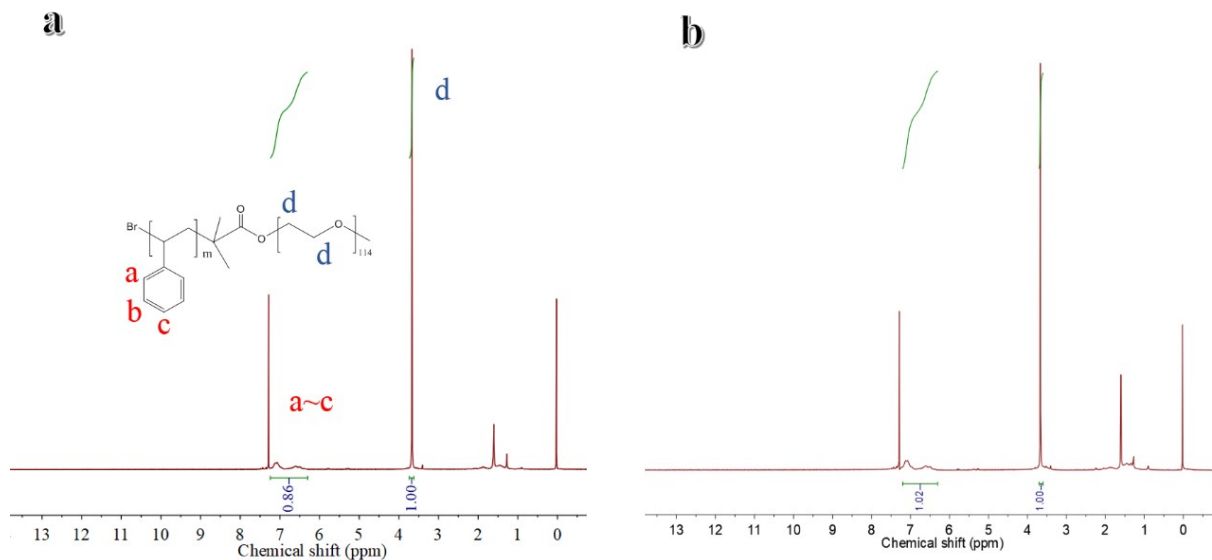


Fig. S4. ¹H NMR spectrum of a) PS₇₈-*b*-PEO₁₁₄ and b) PS₉₃-*b*-PEO₁₁₄. The degree of polymerization (DP) was calculated by the formula. a) DP = $\frac{I_{a-c}/5}{I_d/4} \times 114 = \sim 78$, b) DP = $\frac{I_a/5}{I_b/4} \times 114 = \sim 93$.

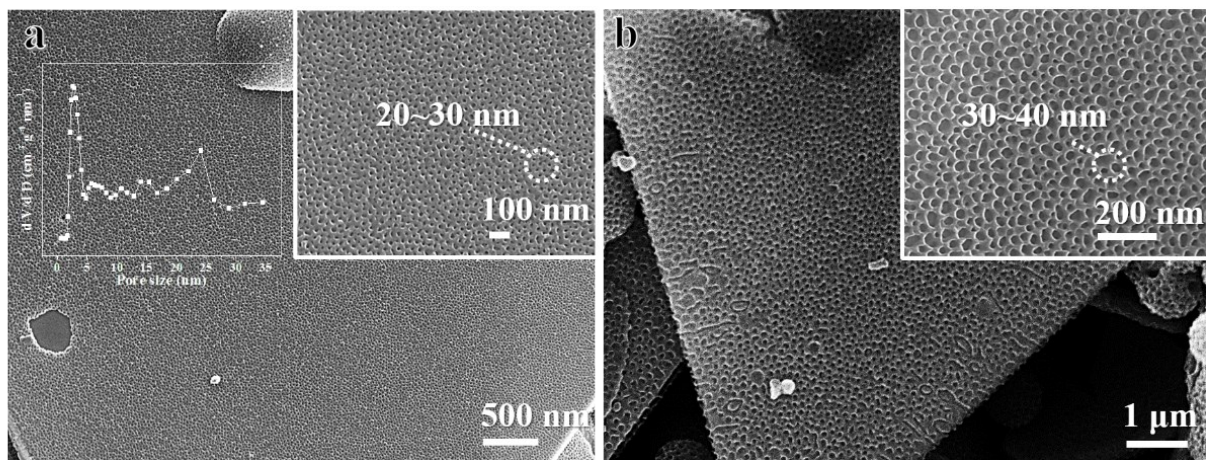


Fig. S5. SEM images of mPPy/Ag prepared by using BCP template of a) $\text{PS}_{78}\text{-}b\text{-PEO}_{114}$ (inset: pore size distribution) and b) $\text{PS}_{93}\text{-}b\text{-PEO}_{114}$.

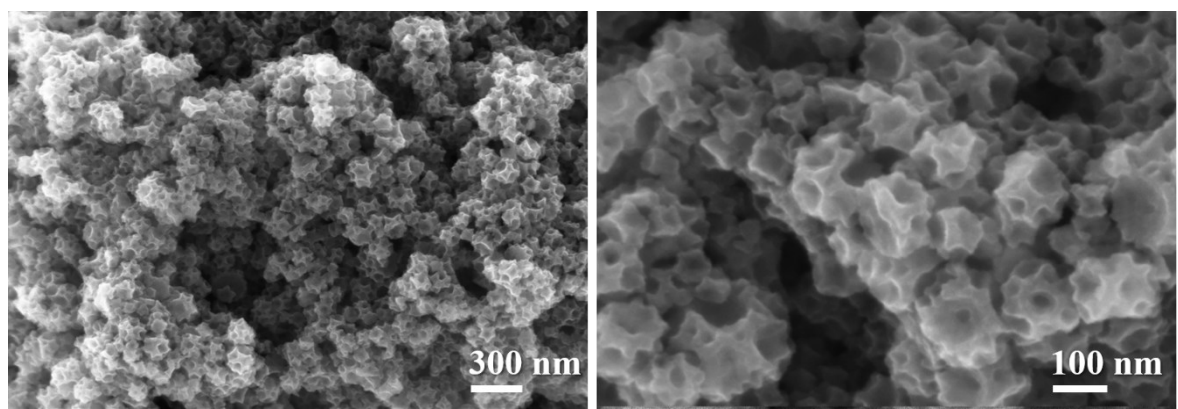


Fig. S6. SEM images of the mPPy/Ag polymerized by ammonium persulfate (APS). Nanospheres with large mesopores (\sim 45 nm) was prepared by the same method in THF/water-chloroform system using ammonium persulfate (APS) as initiator and BCP PS₉₃-*b*-PEO₁₁₄ as template.

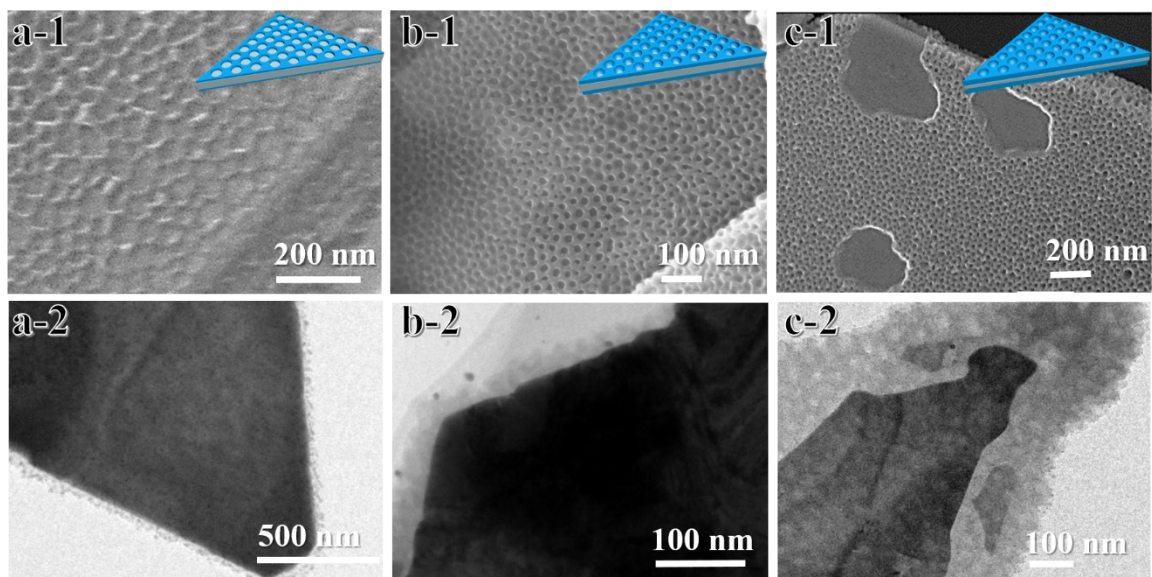


Fig. S7. SEM and TEM images of mPPy/Ag prepared by adjusting the amount of pyrrole monomers of a) 10 μ L, b) 20 μ L, c) 50 μ L.

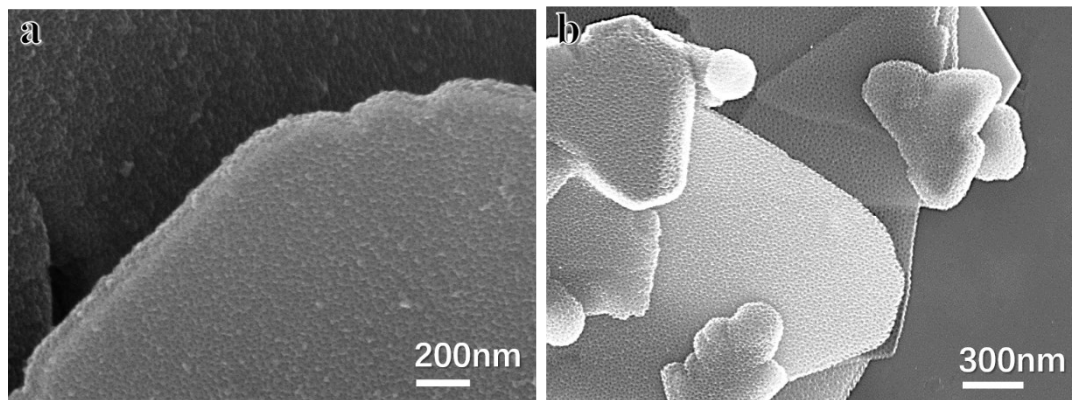


Fig. S8. SEM images of mPPy/Ag samples after being a) exposed to air and b) immersed in ethanol for over a week.

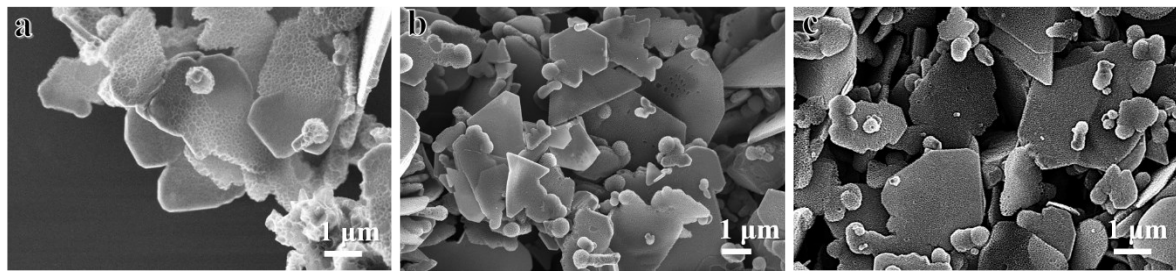


Fig. S9. SEM images of mPPy/Ag samples prepared with different BCP doses, a) 10 mg, b) 25 mg, c) 100 mg.

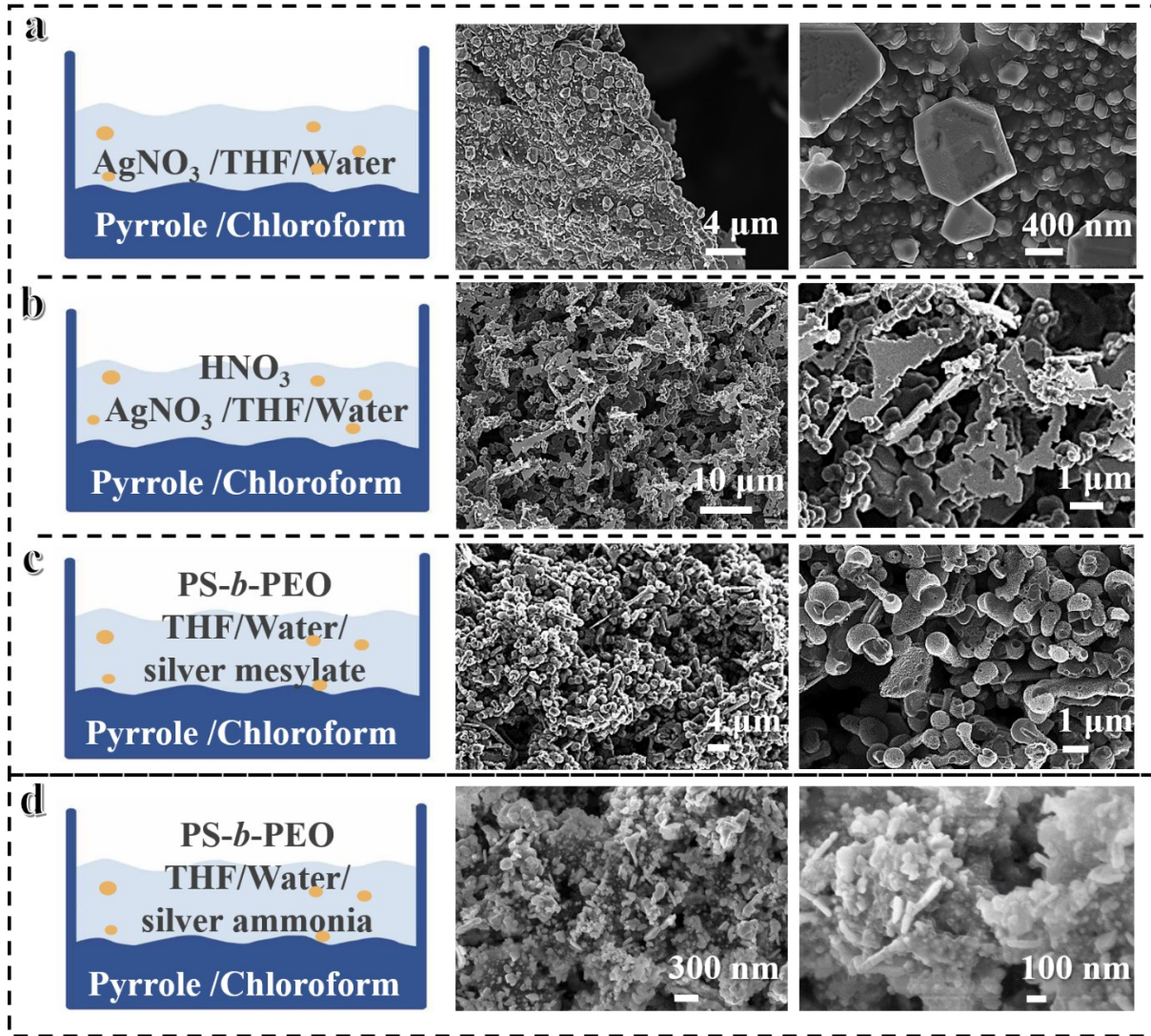


Fig. S10. Schematic diagram and corresponding SEM images for the mPPy/Ag samples of sets of control experiments.

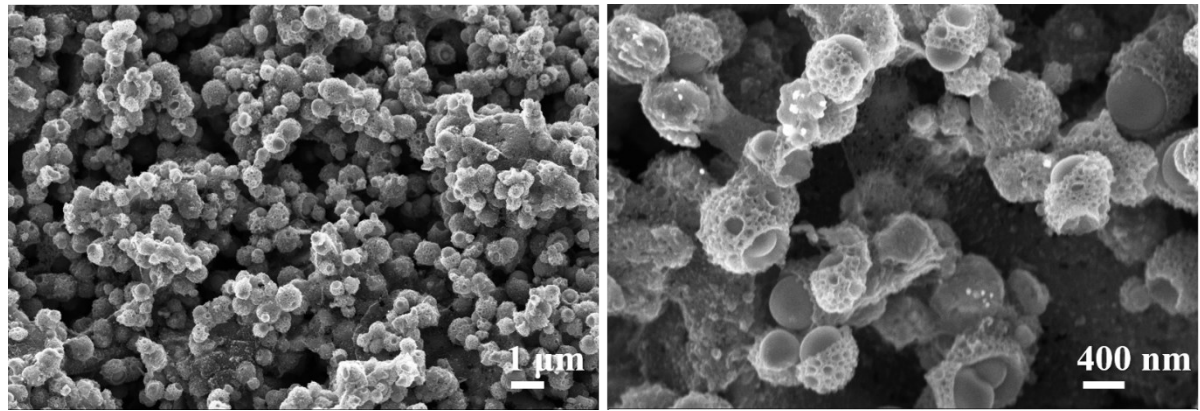


Fig. S11. SEM images of mesoporous PPy@Ag nanospheres samples prepared with mild stirring.

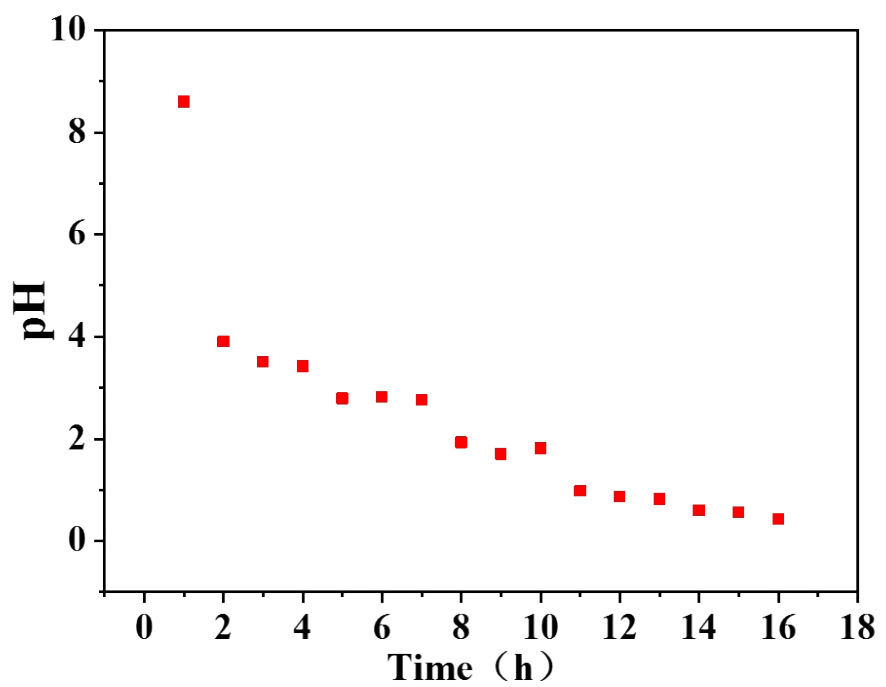


Fig. S12. The image of pH change by hourly monitoring of reaction solution.

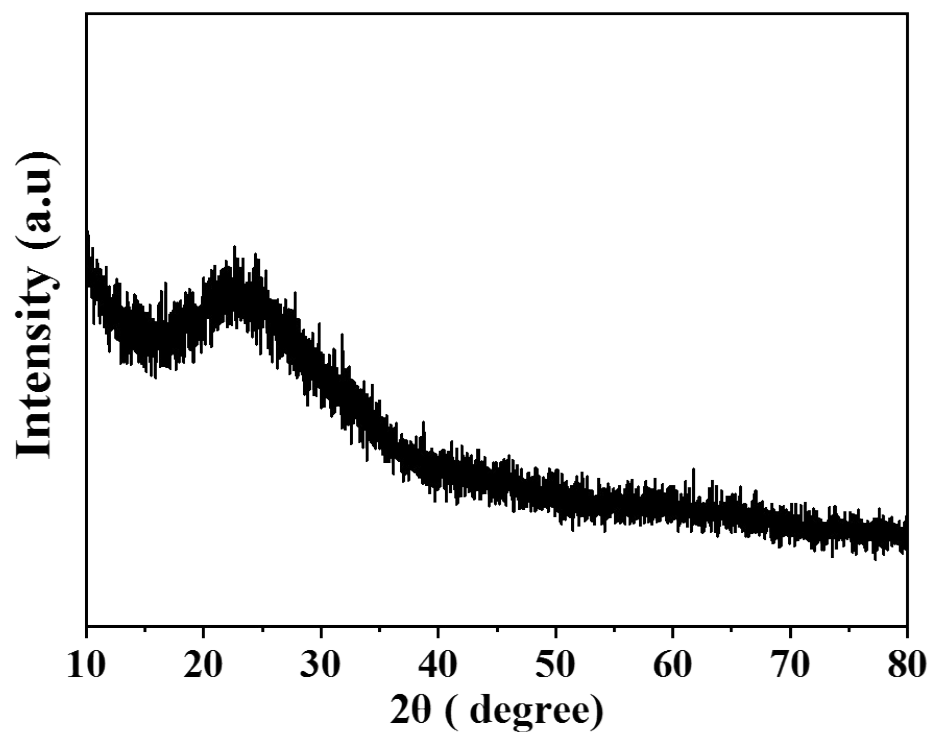
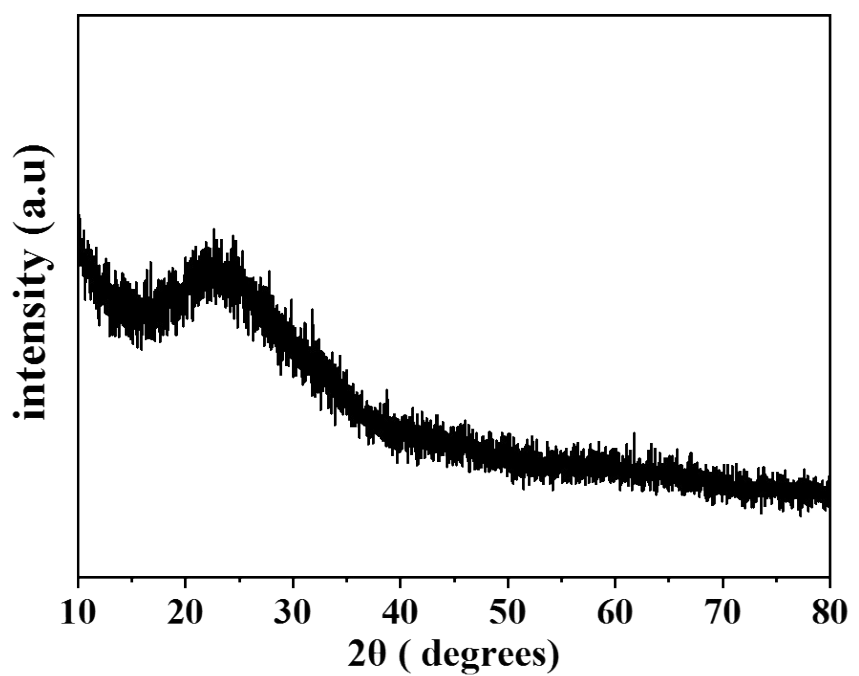


Fig. S13. The XRD spectrum of pure PPy.

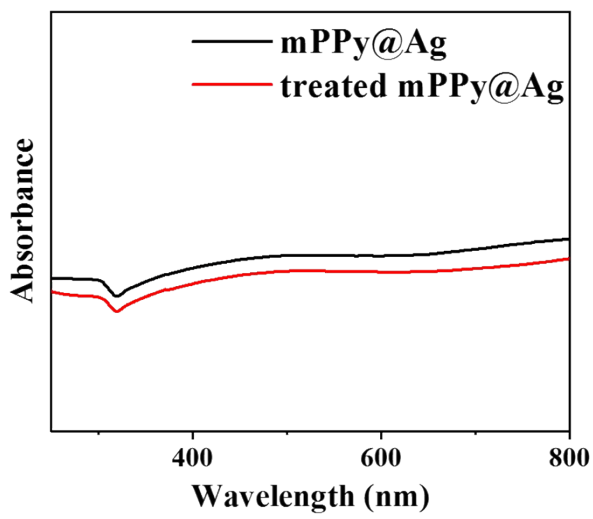


Fig. S14. The UV-VIS-NIR spectra of the as-made mPPy/Ag sample and the treated sample after exposed to air for a week.

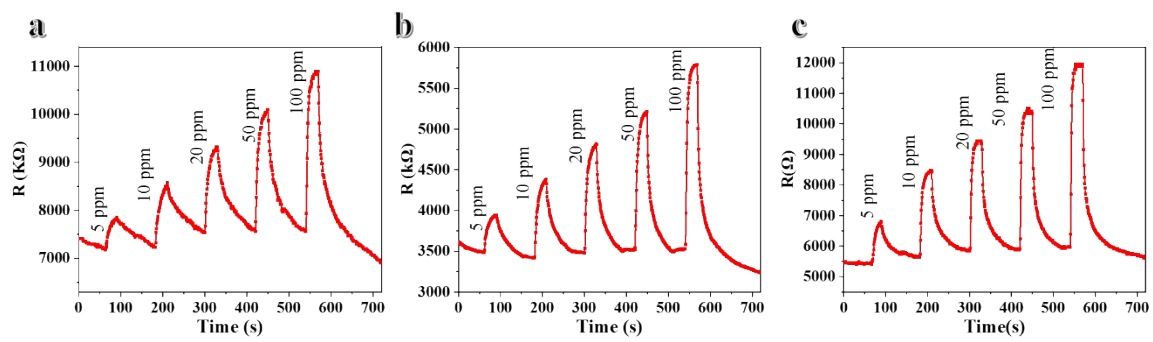


Fig. S15. Response-recovery curves of the a) mPPy sensor and b) bPPy/Ag c) mPPy/Ag-1 sensor in NH₃ at different concentrations of 5-100 ppm.

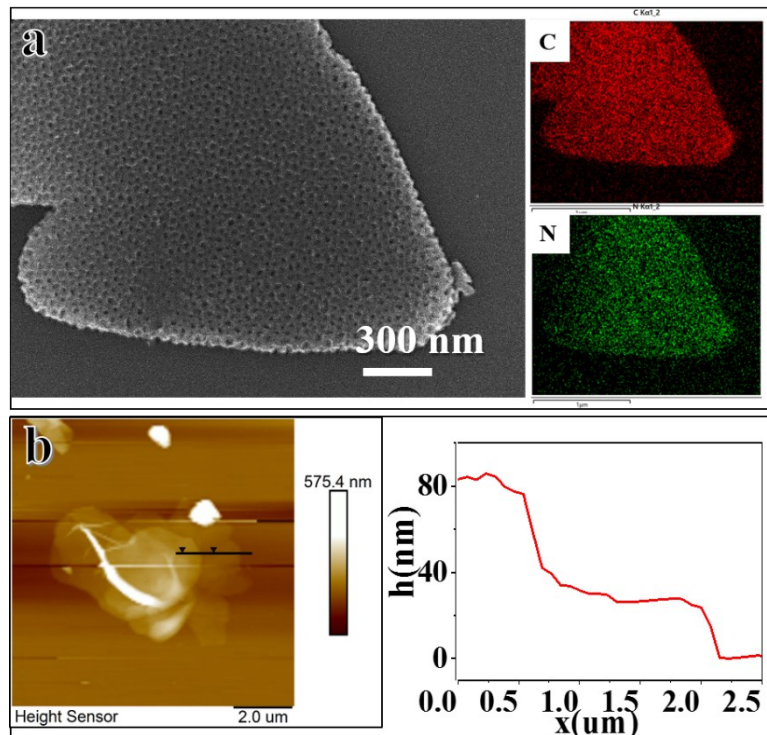


Fig. S16. The a) EDS and b) AFM images of mesoporous PPy sheets prepared by immersing in nitric acid (60°C for 12h) to completely etch Ag nanoplates. The exfoliation of single sheet and the disappearance of Ag elements proved the complete removal of Ag nanoplates, and the thickness of the single-layer mPPy sheet is approximately 30 nm.

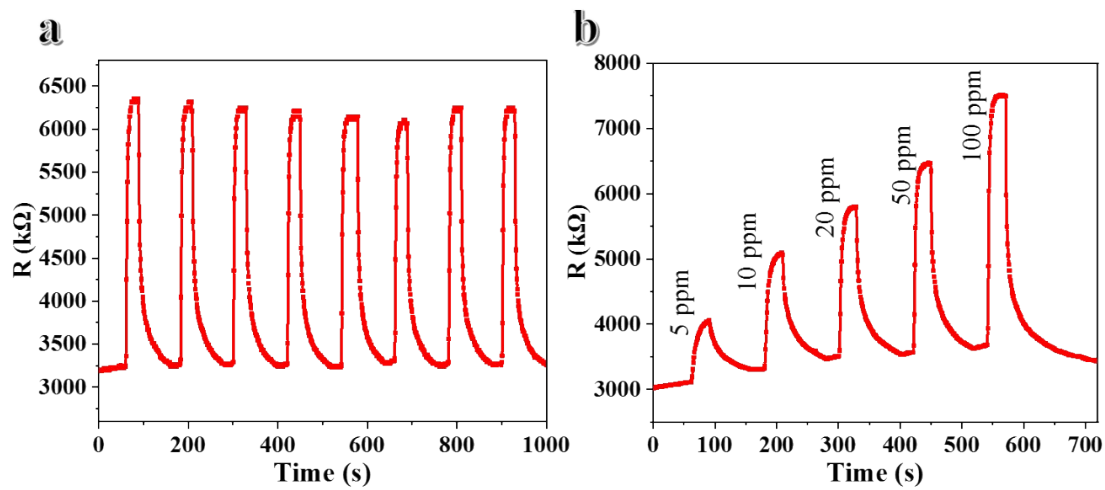


Fig. S17. Response-recovery curves of the a) mPPy/Ag sensor for repeating exposing in 100 ppm NH_3 and b) mPPy/Ag sensor after a week of exposure to air at different concentrations of NH_3

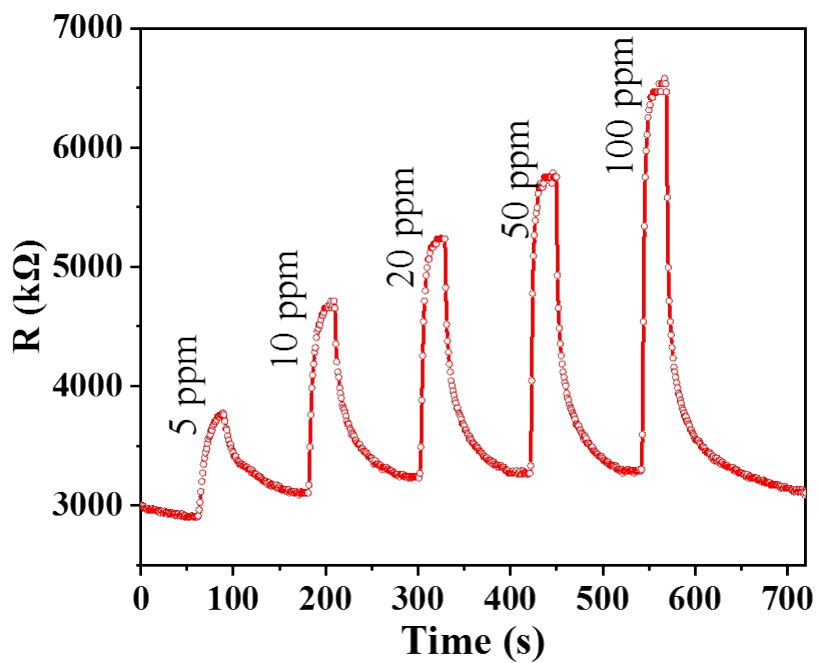


Fig. S18. Response-recovery curve of the flexible PET-based sensor of mPPy/Ag worked at a high bending angles of near 180° at different concentrations of 5-100 ppm NH_3 .

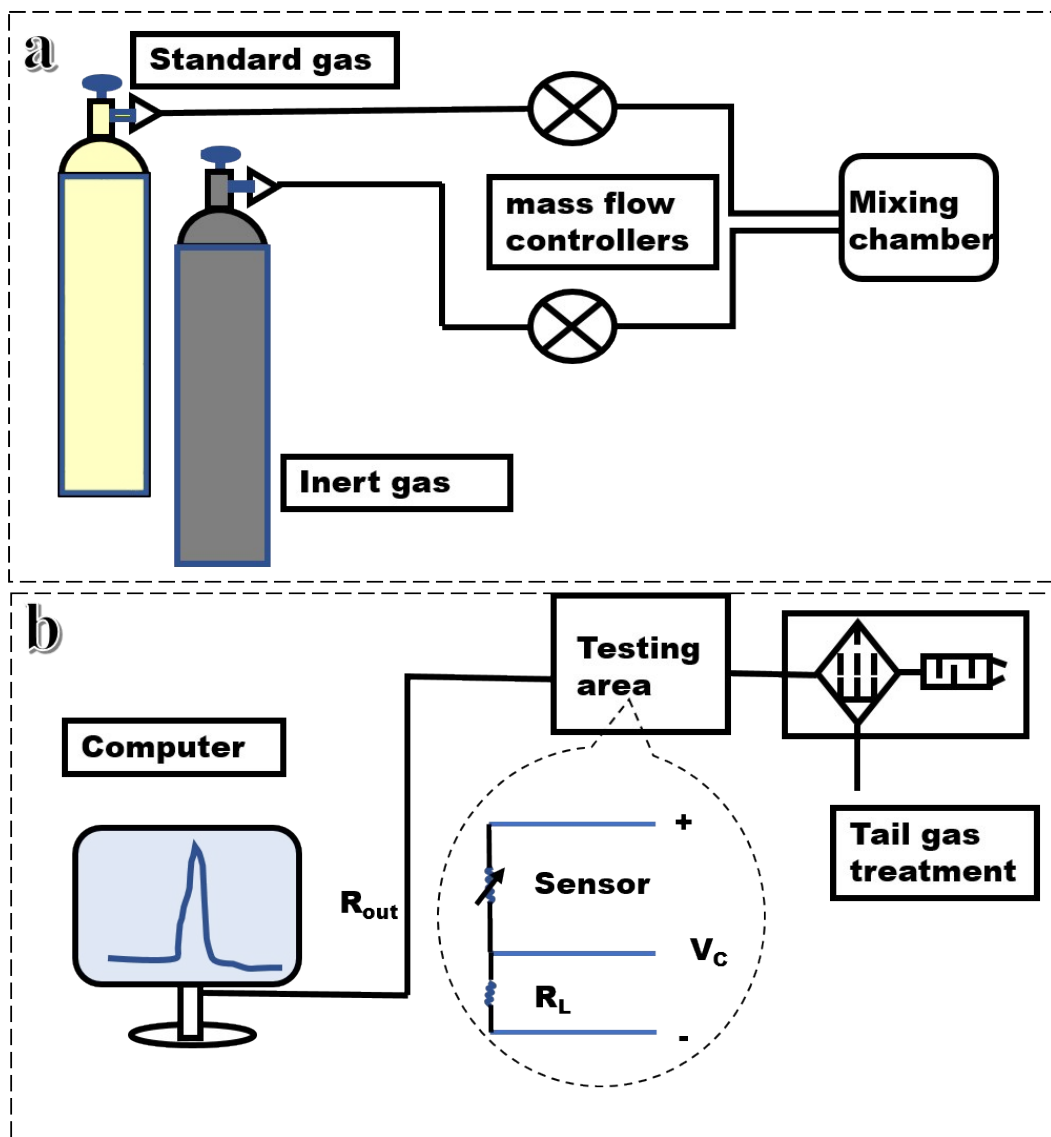


Fig. S19. Sketches of a) gas dilution system and b) gas detection setup.

Table S1. Sensing performance comparison of the mPPy@Ag sensors with previous relevant materials.

Sensing materials	Response (%)	Concentration (ppm)	Response/recovery time (s)
mPPy/Ag nanoplates (this work)	21.2	5	7/21
PPy <u>nanowires</u> ^{s1}	5	100	500/850
PPy/ <u>graphene</u> ^{s2}	10	5	450/600
dual-mesoporous PPy/ <u>graphene</u> ^{s3}	57	40	110/650
multidimensional PPy <u>nanotubes</u> ^{s4}	17	100	1/60
Au/PPy <u>nanopeapods</u> ^{s5}	20	10	15/25*
PPy/rGO <u>composite</u> ^{s6}	6.1	1	60/300
PPy <u>film</u> ^{s7}	31	80	20s/15min
w-mPPy@rGO <u>heterostructures</u> ^{s8}	45	10	200s/10min
Au/PPy nanofibrous <u>film</u> ^{s9}	26.5	100	7/7
PPy-rGO hybrid <u>films</u> ^{s10}	50	10	200*/200*
PPy/Ag composite <u>nanotubes</u> ^{s11}	50	80	200*/500*
mesoporous PPy <u>nanowires</u> ^{s12}	6	100	200/300
SnO ₂ /PPy <u>nanocomposites</u> ^{s13}	53	50	259/468
PPy on single-layered <u>graphene</u> ^{s14}	7.5	1	32/62
Ag nanocrystal-functionalized multiwalled carbon <u>nanotubes</u> ^{s15}	9	10000 (1%NH ₃)	7s/within 5 min (63.2% of the S _{max}).
rGO/ <u>AgNWs</u> ^{s16}	15	100	140/150*

*Estimated values based on the response curve in the reference, others are reported values in the reference.

References:

- S1. D. Kim and B. Yoo, *Sens. Actuators, B*, 2011, **160**, 1168-1173.
- S2. X. Tang, J.-P. Raskin, N. Kryvutsa, S. Hermans, O. Slobodian, A. N. Nazarov and M. Debliquy, *Sens. Actuators, B*, 2020, **305**, 127423.
- S3. J. Qin, J. Gao, X. Shi, J. Chang, Y. Dong, S. Zheng, X. Wang, L. Feng and Z.-S. Wu, *Adv. Funct. Mater.*, 2020, **30**, 1909756.
- S4. O. S. Kwon, S. J. Park, H. Yoon and J. Jang, *Chem. Commun.*, 2012, **48**, 10526-10528.
- S5. Y. Yan, M. Zhang, C. H. Moon, H.-C. Su, N. V. Myung and E. D. Haberer, *Nanotechnology*, 2016, **27**, 325502.
- S6. W. Zhang, G. Li, Y. Chen, S. Liu, J. Xu, C. Jing, J. Zhang, J. Yang, Y. Cheng and J. Chu, *Sens. Actuators, B*, 2020, **305**, 127459.
- S7. A. Joshi, S. A. Gangal and S. K. Gupta, *Sens. Actuators, B*, 2011, **156**, 938-942.
- S8. J. Gao, J. Qin, J. Chang, H. Liu, Z.-S. Wu and L. Feng, *ACS Appl. Mater. Interfaces*, 2020, **12**, 38674-38681.
- S9. Z. Li, J. Chen, L. Chen, M. Guo, Y. Wu, Y. Wei, J. Wang and X. Wang, *ACS Appl. Mater. Interfaces*, 2020, **12**, 55056-55063.
- S10. J. Sun, X. Shu, Y. Tian, Z. Tong, S. Bai, R. Luo, D. Li and C. C. Liu, *Sens. Actuators, B*, 2017, **241**, 658-664.
- S11. X. Yang, L. Li and F. Yan, *Sens. Actuators, B*, 2010, **145**, 495-500.
- S12. I. Rawal and A. Kaur, *Sens. Actuators, A*, 2013, **203**, 92-102.
- S13. Y. Li, H. Ban and M. Yang, *Sens. Actuators, B*, 2016, **224**, 449-457.
- S14. T. Yoon, J. Jun, D. Y. Kim, S. Pourasad, T. J. Shin, S. U. Yu, W. Na, J. Jang and K. S. Kim, *J. Mater. Chem. A*, 2018, **6**, 2257-2263.
- S15. S. Cui, H. Pu, G. Lu, Z. Wen, E. C. Mattson, C. Hirschmugl, M. Gajdardziska-Josifovska, M. Weinert and J. Chen, *ACS Appl. Mater. Interfaces*, 2012, **4**, 4898-4904.
- S16. Q. T. Tran, H. T. M. Hoa, D.-H. Yoo, T. V. Cuong, S. H. Hur, J. S. Chung, E. J. Kim and P. A. Kohl, *Sens. Actuators, B*, 2014, **194**, 45-50.